Molecular Microbiology (2005) **55**(4), 1207–1221 doi:10.1111/j.1365-2958.2005.04457.x

Defence of *Rhizobium etli* bacteroids against oxidative stress involves a complexly regulated atypical 2-Cys peroxiredoxin

Bruno Dombrecht,[1] Christophe Heusdens,[1] Serge Beullens,[1] Christel Verreth,[1] Esther Mulkers,[1] Paul Proost,[2] Jos Vanderleyden[1] and Jan Michiels[1]*

[1]*Centre of Microbial and Plant Genetics, Katholieke Universiteit Leuven, 3001 Heverlee, Belgium.*

[2]*Department of Microbiology and Immunology, Katholieke Universiteit Leuven, 3000 Leuven, Belgium.*

Summary

In general, oxidative stress, the consequence of an aerobic lifestyle, induces bacterial antioxidant defence enzymes. Here we report on a peroxiredoxin of *Rhizobium etli*, *prxS*, strongly expressed under microaerobic conditions and during the symbiotic interaction with *Phaseolus vulgaris*. The microaerobic induction of the *prxS-rpoN*$_2$ operon is mediated by the alternative sigma factor RpoN and the enhancer-binding protein NifA. The RpoN-dependent promoter is also active under low-nitrogen conditions through the enhancer-binding protein NtrC. An additional symbiosis-specific weak promoter is located between *prxS* and *rpoN*$_2$. Constitutive expression of *prxS* confers enhanced survival and growth to *R. etli* in the presence of H_2O_2. Single *prxS* mutants are not affected in their symbiotic abilities or defence response against oxidative stress under free-living conditions. In contrast, a *prxS katG* double mutant has a significantly reduced (>40%) nitrogen fixation capacity, suggesting a functional redundancy between PrxS and KatG, a bifunctional catalase-peroxidase. *In vitro* assays demonstrate the reduction of PrxS protein by DTT and thioredoxin. PrxS displays substrate specificity towards H_2O_2 (K_m = 62 μM) over alkyl hydroperoxides (K_m > 1 mM). Peroxidase activity is abolished in both the peroxidatic (C56) and resolving (C156) cysteine PrxS mutants, while the conserved C81 residue is required for proper folding of the protein. Resolving of the *R. etli* PrxS peroxidatic cysteine is probably an intramolecular process and intra- and intersubunit associations were observed. Taken together, our data support, for the first time, a role for an atypical 2-Cys peroxiredoxin against oxidative stress in *R. etli* bacteroids.

Accepted 1 November, 2004. *For correspondence. E-mail jan.michiels@agr.kuleuven.ac.be; Tel. (+32) 16 329 684; Fax (+32) 16 321 966.

Introduction

The nitrogen-fixing symbiosis between rhizobia and leguminous host plants requires an intensive signal exchange between the two partners (Cullimore *et al*., 2001; D'Haeze and Holsters, 2002; Fraysse *et al*., 2003). Such a rigorous communication allows intracellular infection of the host by the rhizobia.

When a leguminous host plant is infected by rhizobia, the plant produces oxygen species (ROS) like hydrogen peroxide (H_2O_2) and the superoxide anion (O_2^-) at the site of infection (Santos *et al*., 2001). This resembles the hypersensitive response of plants during incompatible plant–pathogen interactions. However, in successful, compatible symbiotic interactions, the rhizobia are able to deal with this host defence response (Mithofer, 2002). Certain rhizobial signal molecules, Nod factors, can inhibit the efflux of ROS from host roots (Shaw and Long, 2003). On the other hand, H_2O_2 appears to be involved in the cross-linking of the matrix glycoprotein in pea infection threads, although only indirect evidence is available (Wisniewski *et al*., 2000). Moreover, H_2O_2 is part of the signalling cascades leading to root nodule formation in *Sesbania rostrata* (D'Haeze *et al*., 2003). In the late stages of symbiosis, the symbiotic metabolism generates an elevated ROS level in the nodules (Becana *et al*., 2000). This mainly results from the elevated respiration rate of bacteroids and mitochondria, the tendency of leghaemoglobin to auto-oxidize, and the abundant presence of O_2-labile proteins, ROS-producing enzymes and non-protein iron. Finally, ROS levels are elevated during nodule senescence.

In order to deal with oxidative stress during the symbiotic interaction, both the host plant and rhizobia have an arsenal of antioxidant tools at their disposal (Becana *et al*., 2000; Herouart *et al*., 2002; Matamoros *et al*., 2003). Like other bacteria, rhizobia possess certain ROS-scavenging enzymes like catalases, superoxide dismutases and peroxidases.

The *Sinorhizobium meliloti* superoxide dismutase *sodA* mutant displays a severely reduced nodulation capacity as well as an impaired bacteroid development and nitrogen fixation capacity (Santos *et al*., 2000). Furthermore, *S. meliloti* possesses two monofunctional catalase-encoding genes, *katA* and *katC*, and one catalase-peroxidase-encoding gene, *katB* (Herouart *et al*., 1996; Sigaud *et al*., 1999; Jamet *et al*., 2003). None of the catalase single mutants shows an altered nodulation or nitrogen fixation capacity, in contrast to the *katA katC* and *katB katC* double mutants (Sigaud *et al*., 1999; Jamet *et al*., 2003). In bacteroids, an increase of catalase activity correlating with KatA induction was observed (Sigaud *et al*., 1999). A proteome analysis of *S. meliloti* revealed that the KatA catalase and SodB superoxide dismutase are abundantly present in bacteroids (Djordjevic *et al*., 2003). Another superoxide dismutase-encoding gene *sodC* appears to be induced during infection (Ampe *et al*., 2003). Oke and Long (1999) described a 1-cysteine peroxiredoxin-encoding gene (*nex1*) of *S. meliloti* that is predominantly expressed in alfalfa root nodules.

In other root nodule bacteria, such as *Rhizobium leguminosarum* bv. *phaseoli*, *R. leguminosarum* bv. *trifolii*, *Bradyrhizobium japonicum* and *Sinorhizobium fredii*, three catalase isoforms could be detected (Crockford *et al*., 1995; Ohwada *et al*., 1999). In contrast to these observations, Vargas *et al*. (2003) found only one catalase-peroxidase (KatG) responsible for catalase and peroxidase activity in *Rhizobium etli* CFN42. However, KatG did not appear to be essential for nodulation or nitrogen fixation in symbiosis with common bean (*Phaseolus vulgaris*). H_2O_2-induced *katG* transcription in CFN42 is most probably mediated by the OxyR regulatory protein.

These enzymes belong to the classic ROS defence arsenal of bacteria. Bacteria respond directly to the presence of oxidative stress by enhancing the expression of ROS detoxifying enzymes. ROS alter the cellular redox status, which in turn activates certain peroxide-sensing regulators (Zheng *et al*., 2001; Mongkolsuk and Helmann, 2002).

Peroxiredoxins (Prxs) are non-haem peroxidases that reduce hydroperoxides at the expense of thiols (Hofmann *et al*., 2002; Wood *et al*., 2003). Prxs have been identified in Eukaryotes, Prokaryotes and Archaea. Members of the Prx superfamily are currently divided into two subgroups, the 1-Cys Prx and the 2-Cys Prx, depending on the presence of one or two conserved cysteine residues. The 2-Cys Prxs possess an N-terminal conserved peroxidatic cysteine (S_p), which is oxidized by peroxides to sulphenic acid (Cys-SOH), and a C-terminal resolving cysteine (S_R). The 2-Cys Prxs have been further subdivided into typical and atypical types, depending on whether the resolving reaction of the Cys-SOH residue occurs through the S_R of a second subunit or with the S_R located within the same subunit respectively (Hofmann *et al*., 2002; Wood *et al*., 2003).

Here we present a combined genetic and biochemical analysis of an atypical 2-Cys peroxiredoxin from *R. etli* that it is specifically and strongly induced during symbiosis with common bean and involved in the defence of *R. etli* bacteroids against hydrogen peroxide stress.

Results

Rhizobium etli *PrxS, an atypical 2-Cys peroxiredoxin*

Rhizobium etli possesses an open reading frame (ORF), directly upstream of and in an operon with *rpoN*$_2$, encoding a peroxiredoxin (179 amino acids, 20 079.9 Da, pI 5.27) (sequence data have been submitted to the DDBJ/EMBL/GenBank databases under Accession No. AJ005696) (Fig. 1). Hereafter, this ORF will be referred to as *prxS* (peroxiredoxin expressed during symbiosis). A BLASTP search (BLOSUM62 similarity matrix) against the non-redundant GenBank databases identified several close homologues of *R. etli* PrxS, which were aligned (Fig. 2). There is a strong overall amino acid conservation [similarity 98–66% (BLOSUM62)/identity 97–47%] between the orthologues. All proteins have at least three cysteine residues, of which the location of two is strictly

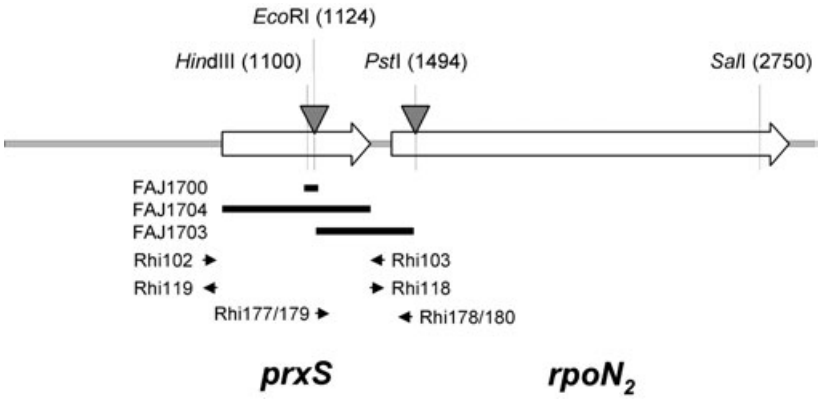

Fig. 1. Physical map of the 2950 bp *R. etli* CNPAF512 *prxS-rpoN*$_2$ region (EMBL Accession No. AJ005696). The Ω-Km insertion sites in FAJ1169 (*rpoN*$_2$), FAJ1170 (*rpoN*$_1$ *rpoN*$_2$), FAJ1173 (*prxS*::Ω-Km) and FAJ1702 (*rpoN*$_1$ *prxS*::Ω-Km) are represented by grey triangles. The black bars represent the deletions of the different mutants. Oligonucleotide primers (small black arrows) are described in *Experimental procedures*.

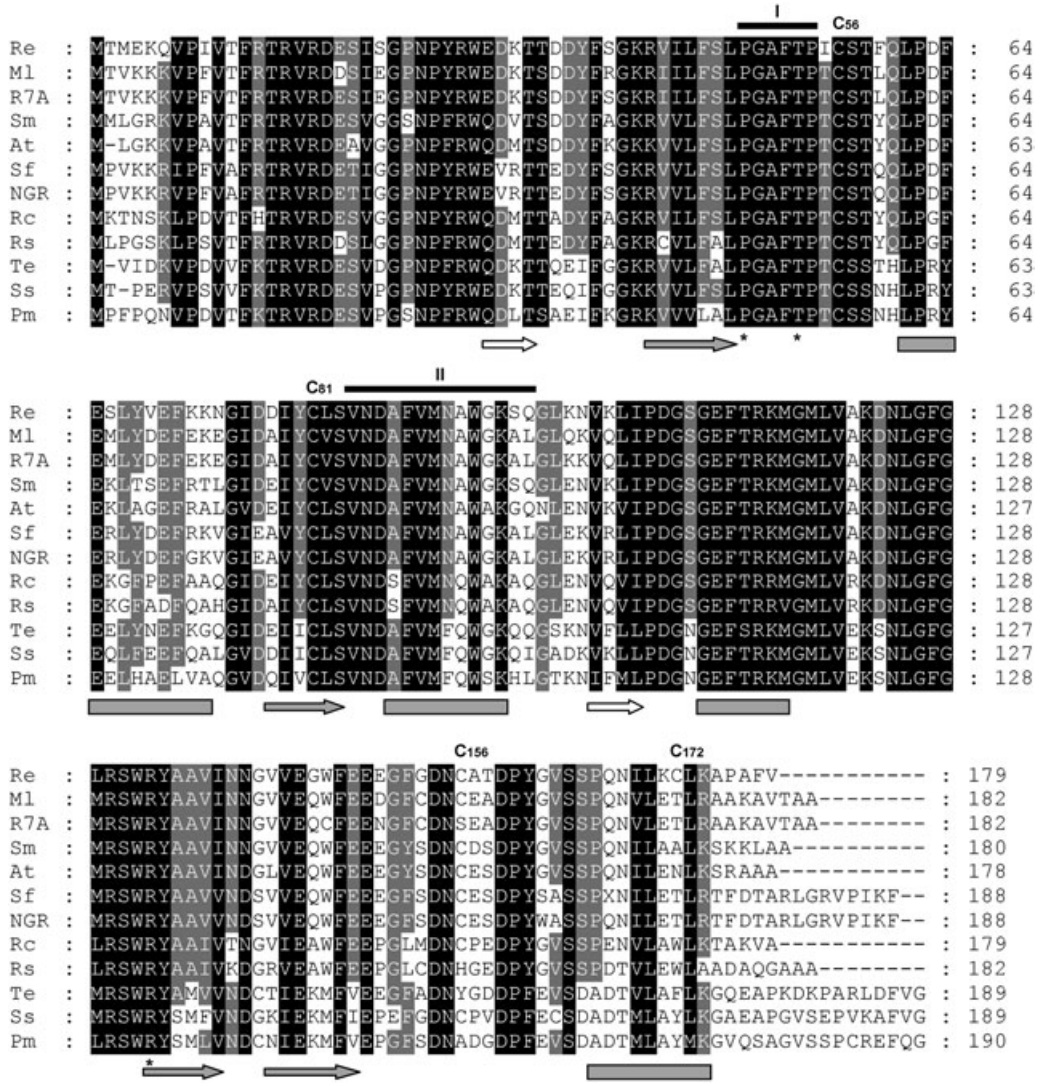

Fig. 2. Alignment of *Rhizobium etli* PrxS orthologues. Re (*R. etli* gi30014171), Ml (*Mesorhizobium loti* MAFF303099 gi13474891), R7A (*M. loti* R7A gi20804163), Sm (*Sinorhizobium meliloti* 15966220), At (*Agrobacterium tumefaciens* gi17936281), Sf (*Sinorhizobium fredii* gi11612206), NGR (*Rhizobium* sp. NGR234 gi16519985), Rc (*Rhodobacter capsulatus* gi7469151), Rs (*Rhodobacter spaeroides* gi22956665), Te (*Trichodesmium erythraeum* gi23041131), Ss (*Synechosystis* sp. PCC 6803 gi16330368) and Pm (*Prochlorococcus marinus* gi33863456). Alignments were performed using CLUSTALW 1.8 (http://searchlauncher.bcm.tmc.edu/multialign/multialign.html). Amino acids are shaded in black (100% conserved) or grey (75% conserved), amino acid similarity according to BLOSUM62. Conserved cysteine residues are marked with a 'C' (numbering is according to the *R. etli* polypeptide). Amino acid residues marked by asterisks are implicated in the activation of the proximal peroxidatic cysteine (Hofmann *et al.*, 2002). Regions I and II (black lines) are necessary for decamer formation, according to Wood *et al.* (2003). Predicted (Jpred: http://www.compbio.dundee.ac.uk/~www-jpred/submit.html; PSIPRED: http://bioinf.cs.ucl.ac.uk/psipred/) conserved α-helices and β-sheets are represented by blocks and arrows, respectively; α-helices and β-sheets that are part of the conserved thioredoxin fold (Wood *et al.*, 2003) are grey.

conserved: C56 and C81. The third cysteine residue is situated around position 156. The *R. etli*, *Mesorhizobium loti* sp. R7A and MAFF303099, *Synechocystis* sp. PCC 6803 and *Prochlorococcus marinus* orthologues have a fourth cysteine residue at their C-terminus. The *Rhodobacter sphaeroides* orthologue also possesses a fourth cysteine residue, although located between the two conserved ones. *In silico* prediction of the secondary structure of PrxS and its orthologues (Fig. 2) reveals a conserved thioredoxin fold, present in all peroxiredoxins (Wood *et al.*, 2003). Several conserved regions and amino acids required for peroxiredoxin function are present as well (Fig. 2). The thioredoxin fold classifies PrxS a member of the Pfam AhpC/TSA protein family (http://www.sanger.ac.uk/cgi-bin/Pfam/getacc?PF00578). Phylogenetic analysis reveals that *R. etli* PrxS belongs to the cluster of atypical 2-Cys peroxiredoxins (http://www.sanger.ac.uk/cgi-bin/Pfam/download_hmm.pl?acc=PF00578&tree=tree&type=full). Comparative three-dimensional modelling, using 3D-Jigsaw (Bates *et al.*, 2001) and Swiss-Model (Schwede *et al.*,

2003), showed an overall strong tertiary structure conservation between *R. etli* PrxS and the peroxiredoxin part of *Haemophilus influenzae* hyPrx5 (Kim *et al*., 2003) and human PrxV (Declercq *et al*., 2001) (the tertiary structure prediction of PrxS is available as supplementary material). Among many other amino acids (36% identity and 55% similarity over 133 amino acids), PrxS shares three conserved cysteine residues with PrxV, the atypical 2-Cys peroxiredoxin archetype (Seo *et al*., 2000). PrxS C56 corresponds to the PrxV C47 peroxidatic cysteine (S_P) and C156 to the PrxV C151 resolving cysteine (S_R). PrxS C81 corresponds to PrxV C72, located at the bottom of the active-site pocket but not required for peroxidatic activity.

prxS *mutant analysis during symbiosis*

Previously, it was reported that a *R. etli prxS* mutant (FAJ1173) fixes the same amount of nitrogen as the *rpoN*$_2$ mutant (FAJ1169) on bean plants grown at 22°C (Michiels *et al*., 1998a). The *R. etli prxS*::Ω-Km mutation has a polar effect on expression of the downstream *rpoN*$_2$ gene, as it could not be complemented *in trans* by the *prxS* gene alone, proving that both genes constitute an operon. When these experiments were repeated at more optimal growth conditions for the bean plants (26°C, medium optimized for bean), a significant difference in nitrogen fixation capacity could be observed between the *rpoN*$_2$ and polar *prxS* mutant (Fig. 3). The *prxS*::Ω-Km mutant has an average residual nitrogenase activity of approximately 60% and the *rpoN*$_2$ mutant of 30%, as compared with the wild type. As the polar *prxS* mutation ends transcription at the insertion site of the Ω-Km interposon, the difference could be explained by the presence of a second promoter downstream of *prxS* and upstream of *rpoN*$_2$. In order to clarify this difference in nitrogen fixation capacity, a *R. etli prxS-rpoN*$_2$ double mutant (FAJ1703) was constructed. The *prxS-rpoN*$_2$ double mutant fixes the same amount of nitrogen as the *rpoN*$_2$ mutant (Fig. 3), demonstrating that the nitrogen fixation phenotype of the *prxS*::Ω-Km mutant results from the polar effect on the downstream *rpoN*$_2$ gene. In addition, this supports the hypothesis of a second promoter directly upstream of *rpoN*$_2$.

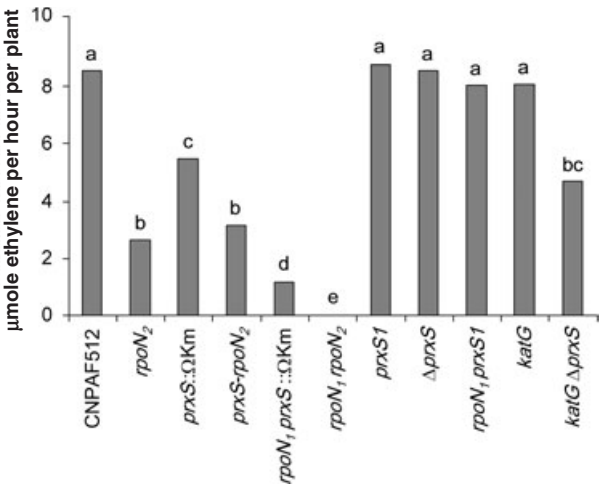

Fig. 3. Acetylene reduction activity of different *R. etli* strains on common bean plant. See *Experimental procedures* for more details on the different strains. Data are means of at least 20 replicates over two independent experiments. Means annotated with different letters are significantly different (Tukey test, $P < 0.05$).

Rhizobium etli possesses two copies of the *rpoN* gene but in contrast to the *rpoN*$_2$ mutant, the *rpoN*$_1$ mutant (FAJ1154) is not impaired in its nitrogen fixation capacity (Michiels *et al*., 1998a). However, *R. etli*'s nitrogen fixation capacity is completely abolished in an *rpoN*$_1$ *rpoN*$_2$ double mutant (FAJ1170) (Fig. 3) (Michiels *et al*., 1998a). To look further into the possibility of a second promoter between *prxS* and *rpoN*$_2$, an *rpoN*$_1$ *prxS*::Ω-Km double mutant was obtained (FAJ1702). Contrary to the *rpoN*$_1$ *rpoN*$_2$ double mutant, the *rpoN*$_1$ *prxS*::Ω-Km double mutant still has a residual nitrogen fixation capacity of 10% (Fig. 3). The presence of a (weak) promoter between *prxS* and *rpoN*$_2$ could account for this observation.

To exclude any downstream effects on *rpoN*$_2$, several non-polar *R. etli prxS* mutants were constructed (see *Experimental procedures*). FAJ1700 and FAJ1701 both harbour the non-polar *prxS* mutant allele *prxS1*, but FAJ1701 has an additional mutation in the first *rpoN* copy, *rpoN*$_1$. The deletion mutant Δ*prxS* (FAJ1704) lacks the complete *prxS* ORF. The *prxS1* and Δ*prxS* mutants did not show a reduction in nitrogenase activity 3 weeks after inoculation, in comparison with the wild-type strain (Fig. 3). An additional knockout of *rpoN*$_1$ in the *prxS1* background did not alter the nitrogen fixation capacity, contrary to the *rpoN*$_1$ *prxS*::Ω-Km double mutant (see above). Complementation of all the tested backgrounds with *prxS in trans* did not alter the nitrogen fixation capacity (data not shown). None of the non-polar *prxS* mutants displayed altered nodulation capacity or kinetics as compared with the wild type (data not shown). In conclusion, the inactivation of *prxS* solely does not affect *R. etli* nitrogen fixation capacity.

The recent description of a plasmid-borne catalase-peroxidase gene, *katG*, in *R. etli* strain CFN42 prompted us to investigate whether such a gene would also be present in *R. etli* strain CNPAF512 and could possibly mask a *prxS* phenotype in symbiosis. CFN42 KatG was shown to be functional and solely responsible for catalase and peroxidase activity although not essential for nodulation and nitrogen fixation (Vargas *et al*., 2003). A *R. etli* CNPAF512 *katG* mutant (FAJ1707) as well as a *katG* Δ*prxS* double mutant (FAJ1708) were constructed. Subsequent determination of the nitrogen fixation capacity on common bean of these strains revealed that the

CNPAF512 *katG* mutant, like the CFN42 *katG* mutant, was still able to fix nitrogen at wild-type levels (Fig. 3). However, the *katG* Δ*prxS* double mutant has a >40% reduction of nitrogen fixation capacity compared with the wild-type strain, demonstrating the need of H_2O_2 detoxification for optimal symbiosis.

Expression analysis of prxS-rpoN$_2$

The expression of *R. etli prxS-rpoN$_2$* is mainly controlled by RpoN-NifA under microaerobic and symbiotic (bacteroid) conditions (Michiels *et al*., 1998a; this work). An additional regulatory mechanism of *prxS-rpoN$_2$* expression is operative only under symbiotic conditions (Michiels *et al*., 1998a). This prompted us to investigate the expression pattern of *prxS-rpoN$_2$* in more detail. High nitrogen availability in the soil has an overall inhibitory effect on the symbiotic interaction between rhizobia and legumes. Low nitrogen availability may fulfil an important signal function for the rhizobia to initiate the symbiosis (Patriarca *et al*., 2002). Therefore, the possible influence of the nitrogen concentration on the expression of the *R. etli prxS-rpoN$_2$–gusA* fusion (pFAJ1175) was assessed. As the *R. etli rpoN$_1$* mutant (FAJ1154) has a reduced capacity to grow on fixed nitrogen sources as compared with the wild type (Michiels *et al*., 1998b), precultures were grown overnight in tryptone-yeast (TY) medium. The precultures were washed twice, diluted twofold in AMS-defined medium (supplied with 10 mM mannitol and 1 mM or 20 mM ammonium) and incubated for 8 h at 30°C. After incubation, the β-glucuronidase activity was determined. A significantly higher expression of pFAJ1175 was found in the wild-type background at 1 mM ammonium as compared with 20 mM (Fig. 4A). This difference is also observed for the *rpoN$_2$* and *nifA* backgrounds, but not for the *rpoN$_1$*, *rpoN$_1$ rpoN$_2$* and *ntrC* (CFN2012) mutants. Apparently, the aerobic induction of *R. etli prxS-rpoN$_2$* by a low nitrogen concentration is dependent on RpoN-NtrC and independent of NifA. A similar, N-dependent expression pattern was observed under microaerobic conditions (Fig. 4B). Overall, the expression levels observed here are higher in comparison with aerobiosis, suggesting a synergism between NtrC and NifA. However, no nitrogen-regulated induction was observed in the *nifA* mutant background. Under symbiotic conditions (in bacteroids), no difference in *prxS-rpoN$_2$* expression was observed between wild-type and *ntrC* mutant backgrounds (data not shown).

Expression of the *prxS-rpoN$_2$* operon thus largely depends on the alternative sigma factor RpoN, acting in conjunction with two enhancer-binding proteins, NifA and NtrC. In order to identify the promoter controlling the operon, the transcription start was mapped, 74 bp upstream of the *prxS* ORF (Fig. 4C and D). Directly upstream of the transcription start site, a highly conserved RpoN binding site (–24/–12 promoter) was found with the conserved G and C at positions –24 and –12 respectively (Fig. 4D). Roughly 300 bp upstream of the transcription start site, putative binding sites for NifA and NtrC could be found.

As most antioxidant defence genes are induced by oxidative stress, we examined the effect of different peroxide concentrations on the expression of the *prxS-rpoN$_2$–gusA* fusion. However, no induction by peroxides was observed (data not shown).

Under free-living microaerobic conditions, the presence of *rpoN$_1$* is required for the NifA-RpoN-dependent expression of *prxS-rpoN$_2$* (Michiels *et al*., 1998a). Only bacteroids of the *R. etli rpoN$_1$* mutant (FAJ1154) are able to initiate the expression of *prxS-rpoN$_2$* in an RpoN-independent manner, after which NifA and RpoN$_2$ maintain the expression of the operon at an elevated level. It therefore appears that a symbiosis-specific condition is required for the RpoN-independent expression of *prxS-rpoN$_2$*. In order to identify this RpoN-independent, symbiosis-specific signalling cascade, we adapted a differential expression assay, previously successfully applied to identify symbiosis-specific genes in *R. etli* (Xi *et al*., 2000; 2001). Briefly, several symbiosis-specific conditions were applied to free-living cultures of the *rpoN$_1$* mutant harbouring a *prxS-rpoN$_2$–gusA* reporter fusion (pFAJ1175) *in trans*. Both microaerobic (Michiels *et al*., 1998a) and/or low-nitrogen conditions (see above) are not sufficient to induce pFAJ1175 in the *rpoN$_1$* mutant. Expression was thus assayed in the presence of nodule extracts, bacteroid extracts, root exudates, flavonoids (naringenin and genistein), dicarboxylic acids as carbon source, different acidic pH conditions (pH 5.0–8.0), low-oxygen and low-nitrogen conditions, and combinations of these. However, no significant induction of pFAJ1175 in the *rpoN$_1$* background could be observed under any of the conditions tested.

The fact that the *R. etli rpoN$_2$* and the *prxS-rpoN$_2$* double mutant display only half of the nitrogen fixation capacity of the *prxS*::ΩKm mutant (see above) suggests the presence of an internal (symbiosis-specific) promoter between *prxS* and *rpoN$_2$*. The same holds true for the 10% remaining nitrogen fixation capacity of the *rpoN$_1$ prxS*::ΩKm double mutant compared with the complete abolishment of nitrogen fixation in the *rpoN$_1$ rpoN$_2$* double mutant (see also above). We cloned the *prxS-rpoN$_2$* intergenic region in both orientations upstream of a *gusA* reporter gene to investigate the possibility of an extra promoter directly upstream of *R. etli rpoN$_2$*. Expression tests showed that there is significantly higher β-glucuronidase activity (50 Miller units) in bacteroids for the fragment in the correct orientation (pFAJ1735) as compared with the opposite orientation (pFAJ1736). This points to the presence of a

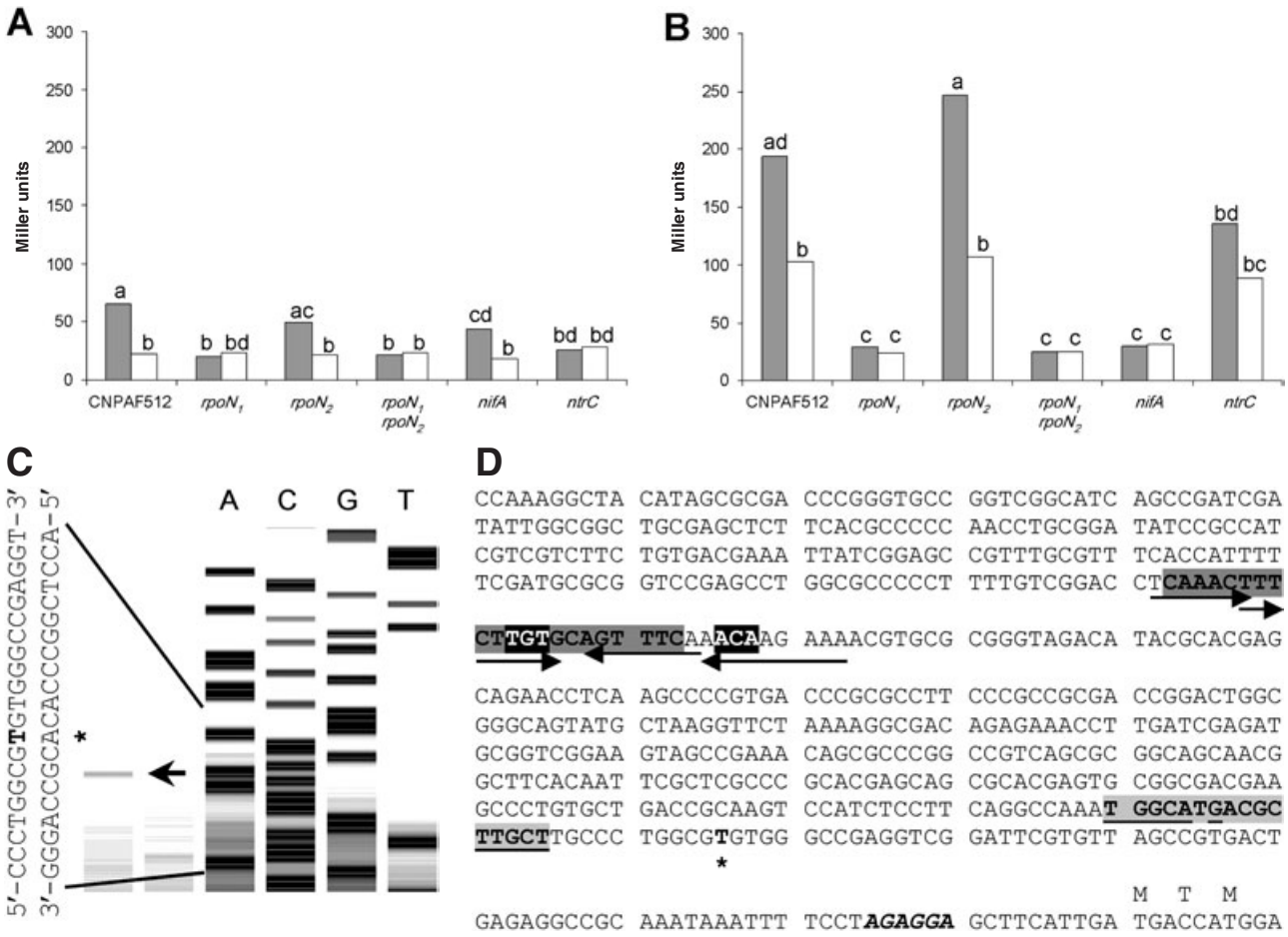

Fig. 4. A and B. Expression analysis of *R. etli prxS-rpoN*$_2$. Free-living expression of *prxS-rpoN*$_2$ (pFAJ1175) under aerobic (A) and microaerobic (0.3% O_2) (B) conditions in different *R. etli* backgrounds. Tests were carried out under low (1 mM, grey bars) or high (20 mM, white bars) ammonium availability. Data are means of at least 12 replicates over six independent experiments. Means annotated with different letters are significantly different (Tukey test, $P < 0.05$).
C. Transcription start mapping of *prxS-rpoN*$_2$. The primer extension was performed on mRNA from microaerobically grown *R. etli* CNPAF512 as described in *Experimental procedures*. The asterisk and arrow mark the transcription start.
D. Promoter region of *prxS-rpoN*$_2$. The first codons of the *prxS* ORF are shown with their respective encoded amino acids, the putative ribosomal binding site is shown in boldface italics and the transcription start is marked with an asterisk. The –24/–12 RpoN binding site (according to Barrios *et al*., 1999) is highlighted in light grey; conserved nucleotides are underlined. Putative NifA and NtrC binding sites are highlighted in black and dark grey respectively. The NtrC binding site was predicted using weight matrix number 52 assembled by Li *et al*. (2002). Arrows represent inverted repeats.

(weak) promoter in the intergenic region, making *R. etli prxS-rpoN*$_2$ a superoperon.

Free-living role for prxS*?*

The symbiotic expression pattern of *R. etli prxS-rpoN*$_2$ complicates the elucidation of the *in vivo* function of PrxS. To overcome this problem, the *R. etli prxS* ORF was cloned downstream the constitutive *nptII* promoter in pFAJ1709, yielding plasmid pFAJ1729 (see *Experimental procedures*). pFAJ1729 was introduced into wild-type *R. etli* CNPAF512. Growth tests were carried out with CNPAF512 and CNPAF512/pFAJ1729 challenged with several ROS, such as H_2O_2, tertiary butyl hydroperoxide (tBuOOH), cumene hydroperoxide (CuOOH) and paraquat to assess whether *prxS* encodes antioxidant activity. Exposure to 2 mM H_2O_2 for 1 h prolongs the lag phase of the cultures with 15 h as compared with the untreated control, reflecting the toxic effect of H_2O_2 (Fig. 5). After a 4 h treatment with 2 mM H_2O_2, no growth could be observed for the wild-type cultures, in contrast to CNPAF512/pFAJ1729 (Fig. 5). Thus, constitutive expression of *prxS* enhances survival of *R. etli* (and *Escherichia coli*, data not shown) on H_2O_2.

Some peroxiredoxins also have alkyl hydroperoxide reductase activity. Although both tBuOOH and CuOOH are toxic to *R. etli*, no enhanced survival or growth as a result of the constitutive expression of *prxS* could be

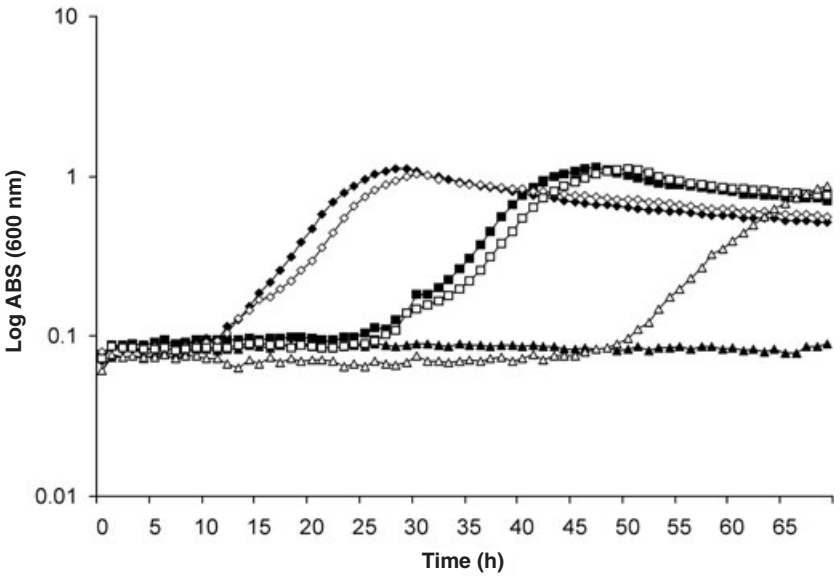

Fig. 5. Growth curves of *R.* etli cultures challenged for 0 (diamonds), 1 (squares) or 4 h (triangles) to 2 mM H_2O_2. Bacterial cultures [CNPAF512 (black symbols), CNPAF512/pFAJ1729 (white symbols)] were grown and treated as described in *Experimental procedures*. Data are representative for three independent experiments.

detected (data not shown). Likewise, the constitutive expression of *prxS* did not alter the toxic effect of paraquat (data not shown).

Although the nitrogen fixation phenotype and expression pattern suggest that *prxS* is predominantly functional during symbiosis, we examined whether *prxS* could also play a role in free-living culture. Several survival experiments in the presence of ROS were undertaken with the Δ*prxS* mutant but no significant difference was detected with the wild-type strain (data not shown). Still, under low-nitrogen conditions, a subtle difference in doubling time appeared to be present between wild-type and Δ*prxS* strains (Table 1). However, this difference was not noticeable in a *katG* background; both *katG* and *katG* Δ*prxS* mutants have equal and considerably prolonged doubling times compared with the wild-type strain.

Taken together, these data suggest that *prxS*, contrary to *katG*, does not play a significant role in *R. etli*'s defence against oxidative stress under free-living conditions.

Overexpression and conformation of PrxS and Cys-Ser mutants

Several T7-overexpression His-tagged constructs for PrxS and Cys-Ser mutants were made (see *Experimental procedures*). Correct translation of the recombinant protein was confirmed by N-terminal sequencing of the first 10 amino acid residues (T-M-E-K-Q-V-P-I-V-T). Figure 6A depicts the purified recombinant wild-type PrxS-His_6 protein under different reducing conditions. As a reduced (50 mM DTT) monomer, PrxS appears as a single band with an apparent molecular weight of 21 kDa, consistent with a predicted weight of 20 902.7 Da (20 079.9 Da without His_6). In non-reducing conditions (absence of DTT), the wild-type protein is present as monomer and dimer (around 42 kDa). Increasing concentrations of DTT result in a gradual loss of the dimeric conformations and in a band shift of the monomeric form. This pattern can be explained by the presence of intra- and intersubunit dicysteine (cystine) bonds in PrxS under non-reducing conditions. Likewise, both C56S and C156S mutants are present in the soluble phase as monomers and dimers, and are able to form inter- and intramolecular cystine bonds under non-reducing conditions (data not shown). In general, native recombinant PrxS protein yields (7 days of IPTG induction at 4°C and purification in the absence of urea) were much lower than under denaturing conditions (4 h of IPTG induction at 37°C and purification in the presence of 8 M urea). When using the standard IPTG induction protocol (4 h at 37°C), all natively harvested recombinant PrxS was present in inclusion bodies (see *Experimental procedures*). Although the PrxS C81S mutant protein could be overexpressed (Fig. 6B) and purified (data not shown) under denaturing conditions, we were unable to obtain any native C81S PrxS. The lack of an overexpres-

Table 1. Doubling times of *R. etli* mutants grown in AMS medium supplied with 10 mM succinate and 10 mM ammonium chloride.

Strain	Genotype	N[a]	Doubling time[b]
CNPAF512	Wild type	345	4 h 51 min*
FAJ1704	Δ*prxS*	349	5 h 07 min†
FAJ1707	*katG*::Ω-Km	249	5 h 29 min‡
FAJ1708	*katG*::Ω-Km Δ*prxS*	249	5 h 28 min‡

a. Number of screened colonies (of four independent experiments).
b. Means annotated with different symbols are significantly different (Tukey test, $P < 0.01$).

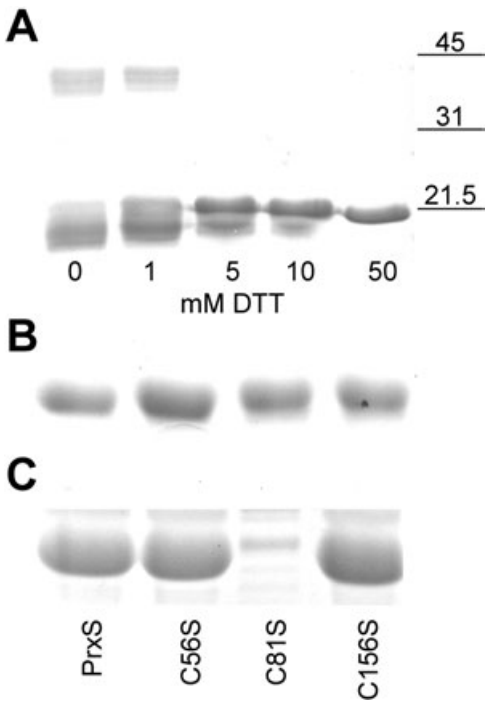

Fig. 6. A. Conformations of recombinant wild-type PrxS. Coomassie stained 12% gel of purified wild-type PrxS separated by non-reducing SDS-PAGE. Purified native PrxS samples were incubated with different concentrations of DTT and heated at 95°C for 5 min. Size markers are indicated in kDa.
B and C. (B) Denatured and (C) natively harvested total soluble fractions of IPTG-induced BL21-CodonPlus(DE3)-RP cells carrying pFAJ1730 (PrxS), pFAJ1745 (C56S), pFAJ1746 (C81S) and pFAJ1747 (C156S) on reducing SDS-PAGE. Samples were prepared as described in *Experimental procedures*.

sion band in the native total soluble phase (Fig. 6C) indicates that the C81S mutant is prone to inclusion body formation, suggesting the involvement of C81 in the stabilization or correct conformation of PrxS.

Peroxidase activity of PrxS

The peroxidase activity of recombinant *R. etli* PrxS-His_6 and Cys-Ser mutants was assayed (Fig. 7A). Wild-type PrxS is able to degrade H_2O_2 in the presence of DTT as a reductant. No H_2O_2 reduction above background levels was observed in the absence of PrxS (2.5 mM DTT) although we observed direct reduction of H_2O_2 at higher DTT concentrations (data not shown). The peroxidatic cysteine (S_P) mutant C56S as well as the resolving cysteine (S_R) mutant C156S are unable to break down H_2O_2 (Fig. 7A). Equimolar mixtures of C56S PrxS and C156S PrxS can not degrade H_2O_2, suggesting that the resolving of the S_P by S_R is an intramolecular process. In search for the *in vivo* reducing agent of *R. etli* PrxS, NADPH oxidation was monitored in the presence of the thioredoxin (TR/Trx/PrxS) and glutaredoxin (GR/GSSG/GRX/PrxS) cascades (see *Experimental procedures*). No activity above background level was observed for the glutaredoxin cascade (data not shown). For the thioredoxin cascade, background levels of NADPH oxidation were measured when any single component of the cascade was omitted. The complete thioredoxin system reduces H_2O_2 (0.64 min^{-1}) although at a slower rate than with DTT (6.20 min^{-1}) as reductant (rates typical for a reaction with 100 μM H_2O_2). Measurements of PrxS activity with varying H_2O_2 concentrations at saturating DTT or NADPH/TR/Trx concentrations gave Michaelis–Menten patterns for both assays (Fig. 7B), with an estimated K_m value of 62.0 μM for H_2O_2 (comparable values were observed for both assays). Parallel experiments using CuOOH and tBuOOH as substrates for PrxS revealed much lower substrate specificities with K_m values of >1 mM and >2 mM respectively (data not shown).

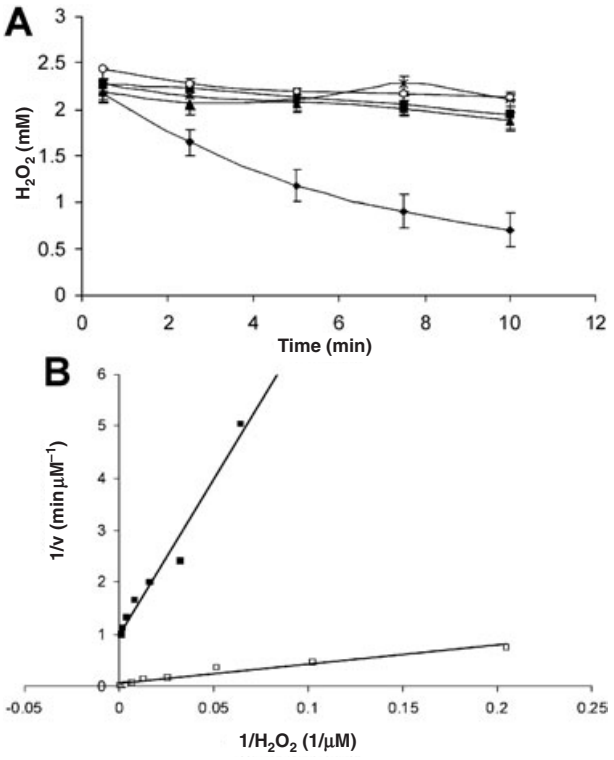

Fig. 7. A. H_2O_2 degradation by recombinant wild-type PrxS and Cys-Ser mutants in the presence of DTT. PrxS (diamonds), C56S (squares), C156S (triangles), equimolar mixture of C56S and C156S (crosses), reaction mixture without PrxS (open circles). Data are means of at least four replicates over three independent experiments; error bars denote standard deviation.
B. Lineweaver–Burke plots of H_2O_2 degradation reactions by PrxS using DTT (open squares) or the thioredoxin cascade (squares) as reductant. Trend lines were fitted by the least squares method. Data are means of at least two independent experiments. Experiments were carried out as described in *Experimental procedures*.

Discussion

Sequence data reveal that the presence of close PrxS orthologues appears to be restricted to rhizobia, *Rhodobacter* spp. and cyanobacteria. In *R. etli*, *Mesorhizobum loti*, *Rhizobium* sp. NGR234 and *S. fredii prxS* lies on the symbiotic genome compartment (SGC) in a nitrogen fixation gene region (Freiberg *et al*., 1997; Michiels *et al*., 1998a; Kaneko *et al*., 2000; Dombrecht *et al*., 2002a; Sullivan *et al*., 2002; Gonzalez *et al*., 2003; gi11612204). An *in silico* analysis predicted the highly conserved RpoN binding site in the promoter region of the *prxS* genes of these species (Dombrecht *et al*., 2002b) suggesting a similar symbiosis-specific gene expression. In fact, the expression of the *Rhizobium* sp. NGR234 *prxS* gene, y4vD, is highly induced in bacteroids (Perret *et al*., 1999). For the two closely related species *S. meliloti* and *Agrobacterium tumefaciens*, the *prxS* gene is located on the chromosome, upstream of the urease-encoding gene loci (Galibert *et al*., 2001; Wood *et al*., 2001). The *Rhodobacter capsulatus* ORF is located in a nitrogen fixation gene region (Schmehl *et al*., 1993). Recently, the requirement of the *Synechocystis* orthologue (*sll1621*) for aerobic phototrophic growth was reported (Kobayashi *et al*., 2004). An *in silico* search with the Pfam AhpC/TSA hidden Markov model (http://www.sanger.ac.uk/cgi-bin/Pfam/getacc?PF00578) revealed that these species have in addition at least three other peroxiredoxins, among which the more generally conserved *E. coli* BCP and AhpC orthologues. This would suggest a highly specialized role for PrxS in these species.

During the initial stages of the interaction, low-nitrogen conditions are required for an optimal symbiotic interaction and could induce *R. etli prxS-rpoN*$_2$ expression through NtrC. At the onset of bacteroid differentiation, *R. etli ntrC* is strongly downregulated (Patriarca *et al*., 1996). At this point, the microaerobic nodule conditions boost *prxS-rpoN*$_2$ expression in a NifA-RpoN-dependent way, providing sufficient RpoN for the expression of the nitrogen fixation genes. Analysis of the *R. etli* CFN42 bacteroid proteome revealed an abundant presence of PrxS (Vargas *et al*., 2003). An alternative RpoN-independent promoter seems to be located in the intergenic region between *prxS* and *rpoN*$_2$. This makes *prxS-rpoN*$_2$ a superoperon, as is the case for *R. capsulatus nifU*$_2$*-rpoN* (Cullen *et al*., 1994). Likewise, a NifA-RpoN-dependent promoter is situated upstream of *nifU*$_2$ with a weak constitutive promoter directly in front of *rpoN*. Most bacterial peroxiredoxin (and other ROS detoxifying) genes are controlled by the OxyR, PerR or OhR regulators that sense peroxides (Zheng *et al*., 2001; Hofmann *et al*., 2002; Mongkolsuk and Helmann, 2002). Here we report, to our knowledge, on the first microaerobically expressed peroxiredoxin gene. Although one would expect less ROS under low-oxygen conditions, apparently there is need for a highly expressed peroxiredoxin in rhizobia under nitrogen-fixing conditions. Being under the control of the RpoN-NifA regulon, *prxS* is coexpressed with the nitrogen fixation genes.

We observed a functional redundancy for *prxS* during symbiosis. A similar hypothesis was put forward by Vargas *et al*. (2003) for the *R. etli katG* gene (and confirmed in this work). The nitrogen fixation phenotype of the *katG* Δ*prxS* double mutant corroborates the PrxS-KatG functional redundancy hypothesis and demonstrates the requirement of *R. etli* PrxS and KatG during symbiosis. For the *S. meliloti* catalases, another symbiotic redundancy was found. The *katA katC* and *katB katC* double mutants display a reduced nodulation capacity, whereas this is not the case for *katA*, *katB* and *katC* single mutants (Sigaud *et al*., 1999; Jamet *et al*., 2003). Although the different *S. meliloti* catalase genes show distinct expression patterns on alfalfa, none of these genes is predominantly expressed during symbiosis, like *R. etli prxS*. Contrary to the *S. meliloti* case, the nitrogen fixation phenotype of the *R. etli* mutants is not the consequence of an altered nodulation capacity but of the specific requirement of PrxS and KatG in the bacteroids, during nitrogen fixation. *R. etli katG* expression is induced by H_2O_2 and is most probably mediated by OxyR (Vargas *et al*., 2003). The fact that *R. etli* KatG is active in bacteroids suggests that H_2O_2 acts as a functional signal in the nodules for rhizobia. Alternatively, a second nodule-specific promoter could act on the *katG* gene. *R. etli* carries (at least) one catalase gene, but in addition maintains a peroxiredoxin gene on its SGC that is abundantly expressed during symbiosis. Such a strategy may not be unexpected as catalases generate O_2 during H_2O_2 dismutation, which may be detrimental for the O_2-sensitive nitrogenase complex.

Phylogenetic analysis and secondary and tertiary structure predictions allocate *R. etli* PrxS to the class of atypical 2-Cys peroxiredoxins. Like all 2-Cys peroxiredoxins, PrxS possesses two highly conserved cysteine residues: a peroxidatic cysteine S_P (C56) and a resolving cysteine S_R (C156). In addition, a third cysteine residue (C81) is absolutely conserved in all the PrxS orthologues, indicative of a significant role. Remarkably, the C81S mutation resulted in the exclusion of *R. etli* PrxS from the native total soluble protein fraction, rendering it more liable to inclusion body formation. This implies that C81 plays an active role in attaining the correct conformation of PrxS. Mutagenesis of the C81 counterpart in mammalian PrxV (C73S) did not alter the peroxidatic activity (Seo *et al*., 2000). A feature that sets PrxS and some of its orthologues apart from other 2-Cys peroxiredoxins is the presence of an additional fourth cysteine residue at their C-terminus. Tertiary structure predictions place C172 at the end of the last helix of the conserved

thioredoxin fold, linked to the rest of the polypeptide by a flexible loop.

Typical 2-Cys peroxiredoxins require the S_R of another subunit to resolve their S_P, whereas for atypical 2-Cys peroxiredoxins the resolving process occurs within the same subunit. Tertiary structure predictions of PrxS point out that C56 is in the near proximity of C156, making the formation of an intramolecular cystine bond likely. Both C56 and C156 are essential for the catalytic cycle of PrxS. Complementation of the C56S with the C156S mutant failed, indicating that the resolving process of the oxidized S_P is an intramolecular process and providing further evidence that PrxS is an atypical 2-Cys peroxiredoxin. Band shift experiments show that PrxS is able to form inter- and intrasubunit disulphide bonds, features of typical and atypical 2-Cys peroxiredoxins respectively. Similar observations were made for the *E. coli* thiol peroxidase (Tpx, p20, scavengase) (Baker and Poole, 2003; Choi *et al*., 2003). Tpx, an atypical 2-Cys peroxiredoxin, operates by an intrasubunit disulphide mechanism but can also be present in solution as a homodimer. PrxS failed to reduce H_2O_2 in assays with the glutaredoxin cascade. Although high glutathione concentrations are found in bacteroids isolated from bean and cowpea nodules (Moran *et al*., 2000), *R. etli* PrxS most probably requires *in vivo* another electron donor. The thioredoxin cascade on the other hand proved to be effective in reducing PrxS, although at low efficiency. Compared with thioredoxin, DTT was approximately 10 times more potent as an electron donor for PrxS. This could mean that the *in vivo* reduction of PrxS occurs through another (dedicated) thiol-dependent oxidoreductase, like for instance the bacterial AhpF homologues known as NADH:peroxiredoxin oxidoreductases (Poole *et al*., 2000). On the other hand, database searches revealed that both the glutaredoxin and thioredoxin pathways are present in rhizobia (http://www.kazusa.or.jp/rhizobase/). It is possible that *R. etli* PrxS does not interact efficiently with the *E. coli* thioredoxin and that it requires the *R. etli* orthologue for successful reduction. PrxS prefers H_2O_2 as a substrate to small alkyl hydroperoxides. This is in line with the observations for the *R. etli* survival/growth experiments with constitutively expressed *prxS* in the presence of different peroxides. The functional redundancy of PrxS and KatG during symbiosis also indirectly suggests that the *in vivo* function of PrxS would be breakdown of H_2O_2.

Taken together, our data support a role for a symbiosis-specific atypical 2-Cys peroxiredoxin in protecting *R. etli* bacteroids against oxidative stress.

Experimental procedures

Bacterial strains and growth conditions

Bacterial strains and plasmids used are listed in Table 2. *E. coli* was routinely grown at 37°C in Luria–Bertani (LB) medium in the presence of the appropriate antibiotics: ampicillin (100 μg ml^{-1}), gentamicin (50 μg ml^{-1}), kanamycin (25 μg ml^{-1}) and spectinomycin (50 μg ml^{-1}). *R. etli* was cultured at 30°C in liquid TY medium (supplemented with 7 mM $CaCl_2$) or in liquid-defined acid minimal salts (AMS) medium (Poole *et al*., 1994) (supplemented with nitrogen and carbon sources) and stored on yeast extract mannitol (YEM) (Vincent, 1970) agar plates. The following antibiotics were used: nalidixic acid (30 μg ml^{-1}), neomycin (30 μg ml^{-1}), spectinomycin (25 μg ml^{-1}) and tetracycline (1 μg ml^{-1}).

DNA constructs

Mutants. A non-polar *R. etli prxS* mutant, *prxS1* (FAJ1700), was constructed as follows. A *Hin*dIII–*Eco*RI adaptor fragment, containing a *Sal*I restriction site and stop codons in the three reading frames, was obtained by hybridization of primers BD02 (5′-AGCTT**TGA**C**TAG**C**TAA**GTCGACG-3′; the *Sal*I restriction site is underlined and the stop codons are in boldface) and BD03 (5′-AATTCGTCGAC**TTA**G**CTA**G**TCA**A-3′; the *Sal*I restriction site is underlined and the stop codons are in boldface). The adaptor fragment was ligated into *Hin*dIII–*Eco*RI-digested pFAJ1174, yielding pFAJ1721. The correct insertion of the adaptor was confirmed by determination of the nucleotide sequence. The insertion results in a non-polar mutation of *R. etli prxS* caused by a frame shift in the ORF, a deletion of 18 bp from the ORF and the presence of stop codons in the three reading frames. The *Not*I fragment of pFAJ1721 was cloned into *Not*I-digested pJQ200SK, resulting in pFAJ1722.

A *R. etli prxS* deletion mutant, Δ*prxS* (FAJ1704), was obtained as follows. An inverse polymerase chain reaction (PCR) was performed on pFAJ1174 with Platinum *Pfx* DNA polymerase and primers Rhi118 (5′-GCATTGAAGCCAAC GACCAGC-3′) and Rhi119 (5′-CAATGAAGCTCCTCTAGG AAAATTTATTTGCGG-3′). The 6.3 kb PCR product, pFAJ1174 lacking the *prxS* ORF, was ligated, giving rise to pFAJ1731. The correct deletion of the *R. etli prxS* ORF was confirmed by nucleotide sequencing. The *Not*I fragment of pFAJ1731 was ligated into *Not*I-digested pJQ200SK, yielding pFAJ1732.

A *R. etli prxS-rpoN$_2$* double mutant (FAJ1703) was constructed as follows. A 370 bp *Eco*RI–*Pst*I fragment, comprising the 3′ region of *prxS* and the 5′ region of *rpoN$_2$*, was deleted from pFAJ1174. The truncated plasmid was blunted with T4 DNA polymerase and ligated to an Ω-Km cassette (Fellay *et al*., 1987), thereby inactivating both *prxS* and *rpoN$_2$*. The correct insertion of the Ω-Km cassette (in the opposite orientation as *prxS-rpoN$_2$*) in the resulting plasmid, pFAJ1723, was confirmed by restriction analysis and DNA sequence determination. The *R. etli prxS-rpoN$_2$* mutant fragment was cut out of pFAJ1723 with *Not*I and subsequently ligated into *Not*I-digested pJQ200SK, yielding pFAJ1724.

A *R. etli* CNPAF512 *katG* mutant (FAJ1707) was constructed as follows. The complete CNPAF512 *katG* gene was amplified using *Taq* DNA polymerase from genomic DNA with primers based on the *R. etli* CFN42 *katG* sequence: Rhi589 (5′-GTACGCGGCCGCAAGCCGA GCTTATCGCAGC-3′; the *Not*I restriction site is underlined) and Rhi590 (5′-GTACGCG GCCGCGCAAAATTGGCGGAACCG-3′; the *Not*I restriction site is underlined). The 2.3 kb PCR product obtained was

Table 2. Bacterial strains and plasmids.

Strain or plasmids	Relevant properties	Source or reference
Strains		
E. coli		
DH5α		Gibco BRL
BL21-	B F– *ompT hsdS*(rB– mB–) *dcm*+ Tet^r	Stratagene
CodonPlus(DE3)-RP	*gal*I (DE3) *endA* Hte [*argu proL* Cam^r]	
R. etli		
CFN2012	*ntrC*::Tn*5* derivative of *R. etli* CFN42	Moreno *et al*. (1992)
CNPAF512	Nal^r, wild type	Michiels *et al*. (1998b)
Rp1000	Nal^r Nm^r *nifA*::*aphII*	Michiels *et al*. (1994)
FAJ1154	Nal^r Nm^r *rpoN*$_1$::Ω-Km	Michiels *et al*. (1998b)
FAJ1169	Nal^r Nm^r *rpoN*$_2$::Ω-Km	Michiels *et al*. (1998a)
FAJ1170	Nal^r Sp^r Nm^r *rpoN*$_1$::Ω-Sp *rpoN*$_2$::Ω-Km	Michiels *et al*. (1998a)
FAJ1173	Nal^r Nm^r *prxS*::Ω-Km	Michiels *et al*. (1998a)
FAJ1700	Nal^r *prxS1* (non-polar *prxS* mutant)	This work
FAJ1701	Nal^r Sp^r *rpoN*$_1$::Ω-Sp *prxS1*	This work
FAJ1702	Nal^r Sp^r Nm^r *rpoN*$_1$::Ω-Sp *prxS*::Ω-Km	This work
FAJ1703	Nal^r Nm^r *prxS-rpoN*$_2$::Ω-Km	This work
FAJ1704	Nal^r Δ*prxS*	This work
FAJ1707	Nal^r Nm^r *katG*::Ω-Km	This work
FAJ1708	Nal^r Nm^r *katG*::Ω-Km Δ*prxS*	This work
Plasmids		
pBluescriptII-SK+	Ap^r	Stratagene
pCRII-TOPO	Ap^r Km^r	Invitrogen
pCR4Blunt-TOPO	Ap^r Km^r	Invitrogen
pET-24(+)	Km^r plasmid for T7 overexpression of protein-His Tag fusions	Novagen
pHP45-ΩKm	Ap^r Nm^r Ω-Km	Fellay *et al*. (1987)
pJQ200SK	Gm^r *sacB* p15A replicon	Quandt and Hynes (1993)
pRK2073	Sp^r ColE1 helper plasmid for triparental mating	Figurski and Helinski (1979)
pFAJ1174	April 4.2 kb *Not*I fragment containing *prxS* and *rpoN*$_2$ cloned in pUC18Not	Michiels *et al*. (1998a)
pFAJ1175	Tc^r *rpoN*$_2$–*gusA* fusion in pLAFR3	Michiels *et al*. (1998a)
pFAJ1186	Gm^r Sp^r pJQ200-UC1 containing *rpoN*$_1$::Ω-Sp	Michiels *et al*. (1998a)
pFAJ1703	Ap^r Tc^r *gusA* stable RK2-derived promoter probe vector	Dombrecht *et al*. (2001)
pFAJ1709	Ap^r Tc^r RK2-derived constitutive expression vector harbouring *nptIIp*	Dombrecht *et al*. (2001)
pFAJ1711	April 2.3 kb PCR fragment containing *katG* cloned in pCRII-TOPO	This work
pFAJ1713	Gm^r 1.7 kb *Not*I fragment of pFAJ1711 containing part of *katG* cloned in pJQ200UC1	This work
pFAJ1714	Gm^r Km^r pJQ200-UC1 containing *katG*::Ω-Km	This work
pFAJ1721	Ap^r disruption of the *prxS* ORF from pFAJ1174	This work
pFAJ1722	Gm^r pJQ200SK containing *Not*I fragment bearing non-polar mutation of *prxS* from pFAJ1721	This work
pFAJ1723	Ap^r Nm^r Ω-Km cassette cloned oppositely to the orientation of the *prxS-rpoN*$_2$ ORFs into *Eco*RI–*Pst*I cut pFAJ1174	This work
pFAJ1724	Gm^r Nm^r pJQ200SK containing *Not*I fragment bearing *prxS-rpoN*$_2$::Ω-Km from pFAJ1723	This work
pFAJ1729	Ap^r Tc^r pFAJ1709 containing *prxS*	This work
pFAJ1730	Km^r wild-type PrxS in pET-24(+)	This work
pFAJ1731	Ap^r pFAJ1174 lacking the complete *prxS* ORF	This work
pFAJ1732	Gm^r pJQ200SK containing *Not*I fragment bearing *prxS* deletion from pFAJ1731	This work
pFAJ1733	Ap^r *prxS-rpoN*$_2$ intergenic region (correct orientation) in pCR4Blunt-TOPO	This work
pFAJ1734	Ap^r *prxS-rpoN*$_2$ intergenic region (opposite orientation) in pCR4Blunt-TOPO	This work
pFAJ1735	Ap^r Tc^r *prxS-rpoN*$_2$ intergenic region (correct orientation) cloned *Bam*HI–*Xba*I into pFAJ1703	This work
pFAJ1736	Ap^r Tc^r *prxS-rpoN*$_2$ intergenic region (opposite orientation) cloned *Bam*HI–*Xba*I into pFAJ1703	This work
pFAJ1739	Ap^r *prxS* ORF cloned *Bam*HI–*Xho*I into pBluescriptII-SK+	This work
pFAJ1745	Km^r C56S PrxS in pET-24(+)	This work
pFAJ1746	Km^r C81S PrxS in pET-24(+)	This work
pFAJ1747	Km^r C156S PrxS in pET-24(+)	This work

cloned into pCRII-TOPO (pFAJ1711) and correct amplification was confirmed by DNA sequence determination. A 1.7 kb *Not*I fragment, encompassing the last two-thirds of *katG*, was ligated into pJQ200UC1 (pFAJ1713). Then, the Ω-Km cassette (Fellay *et al*., 1987) was cloned in the opposite orientation into *Bam*HI digested pFAJ1713, giving rise to a *katG* knockout construct: pFAJ1714.

All suicide constructs were introduced into the *R. etli* CNPAF512 wild-type background by double homologous recombination. Correct insertion of the mutations was confirmed by Southern hybridization and/or PCR.

The *katG* suicide construct was also introduced into the Δ*prxS* mutant background (FAJ1704), resulting in a *katG-prxS* double mutant (FAJ1708). Two *R. etli prxS rpoN*$_1$ double

mutants, FAJ1701 and FAJ1702, were generated from non-polar *prxS1* (FAJ1700) and polar *prxS*::Ω-Km (FAJ1173) mutant backgrounds, respectively, by introduction of an $rpoN_1$ suicide construct (pFAJ1186).

Other constructs. A constitutively expressed construct of *R. etli prxS* was made for functional analysis. *prxS* was amplified from total genomic wild-type CNPAF512 DNA with Pwo DNA polymerase and primers Rhi102 (5′-AGTCTCTAGAACCGT GACTGAGAGGCCGC-3′; the *Xba*I restriction site is underlined) and Rhi103 (5′-AGTCGG TACCTCATTCGGCGCA GGTGTG-3′; the *Kpn*I restriction site is underlined). The resulting 650 bp product was digested with *Kpn*I and *Xba*I and subsequently ligated into *Kpn*I–*Xba*I-treated pFAJ1709 (Dombrecht *et al*., 2001), yielding pFAJ1729. pFAJ1729 harbours the *R. etli prxS* ORF under the control of the *nptII* promoter.

The *prxS-rpoN*$_2$ intergenic region was amplified from genomic DNA with Platinum *Pfx* DNA polymerase and primers Rhi177 (5′-ATCGGGATCCCTCGGAAAATGGGTATGC-3′; the *Bam*HI site is underlined) and Rhi178 (5′-ACGTTCT AGACAAGCGAATAGACGCGATGAGC-3′; the *Xba*I site is underlined) and ligated into pCR4Blunt-TOPO (pFAJ1733); and with primers Rhi179 (5′-ATCGTCTAGACTCGGAAAAT GGGTATGC-3′; the *Xba*I site is underlined) and Rhi180 (5′-ACGTGGATCCCAAGCGAATAGACGCGATGAGC-3′; the *Bam*HI site is underlined) and ligated into pCR4Blunt-TOPO (pFAJ1734). The correct amplification of the fragments was confirmed by nucleotide sequencing. The products were cut out (*Bam*HI–*Xba*I) and ligated into *Bam*HI–*Xba*I-treated pFAJ1703 (Dombrecht *et al*., 2001), resulting in transcriptional fusions of *gusA* and the *prxS-rpoN*$_2$ intergenic fragment in the correct (pFAJ1735) and opposite (pFAJ1736) orientation.

Site-directed mutagenesis of prxS. *Rhizobium etli* CNPAF512 *prxS* was amplified from genomic DNA with Pwo DNA polymerase and primers Rhi114 (5′-ACTCGGATC CAATAATTTTGTTTAACTTTAAGAAGGAGATATACAT**ATG**AC CATGGAAAAGCAGGTCCCTATTGTCACC-3′; the *Bam*HI restriction site is underlined, the *prxS* start codon is in boldface) and Rhi115 (5′-ATCGCTCGAGTACGAAGGCTGG GGCCTTAAGGC-3′; the *Xho*I restriction site is underlined). The resulting PCR product was digested with *Bam*HI and *Xho*I and cloned into *Bam*HI–*Xho*I-treated pBluescript II SK+, giving rise to pFAJ1739.

Cysteine to serine mutants of PrxS were obtained by inverse PCR on pFAJ1739 with Platinum *Pfx* DNA polymerase and different sets of mismatch primers. The mutations were confirmed by DNA sequencing after which the mutated ORFs were transferred as *Bam*HI–*Xho*I fragments into pET-24(+). The following primer sets were used: C56S, Rhi367 (5′-CCTTCACGCCAATCTCCTCCACCTTCCAACT GC-3′; the mismatch site is underlined) and Rhi368 (5′-GCAGTTGGAAGGTGGAGGAGATTGGCGTGAAGG-3′; the mismatch site is underlined); C81S, Rhi369 (5′-GCATTGAC GACATCTACTCTCTCTCCGTCAACG-3′; the mismatch site is underlined) and Rhi370 (5′-CGTTGACGGAGAGAGAGTA GATGTCGTCAATGC-3′; the mismatch site is underlined); C156S, Rhi371 (5′-GGCTTTGGCGACAACTCCGCGACCG ATCCG-3′; the mismatch site is underlined) and Rhi372 (5′-CGGATCGGTCGCGGAGTTGTCGCCAAAGCC-3′; the mismatch site is underlined).

The correct amplification of the different products was confirmed by DNA sequencing. Next, they were cloned (*Bam*HI–*Xho*I) in frame and in front of six His codons followed by a stop codon in pET-24(+): pFAJ1730 (wild-type PrxS), pFAJ1745 (C56S PrxS), pFAJ1746 (C81S PrxS) and pFAJ1747 (C156S PrxS).

β-Glucuronidase assays and non-radioactive primer extension

Expression tests, using *p*-nitrophenyl-β-D-glucuronide (Sigma-Aldrich, St Louis, MO, USA) as a substrate for the β-glucuronidase, were carried out as described earlier (Michiels *et al*., 1998a).

RNA (100 μg) was extracted from a microaerobic *R. etli* culture following the phenol-extraction procedure as described by Eggermont *et al*. (1996). The RNA was mixed with 20 pmol of primer BD-43 (5′-CGCTGAAATAGTCGTCG GTC-3′, labelled with a fluoresceine group at the 5′-end) and precipitated overnight at −20°C in 300 mM NaOAc and 70% (v/v) ethanol. The pellet was redissolved in hybridization buffer [80% (v/v) formamide, 40 mM PIPES pH 6.8, 400 mM NaCl, 1 mM EDTA] and allowed to hybridize overnight at 30°C after a 10 min denaturation step at 85°C. After another overnight precipitation (see above), the pellet was washed [70% (v/v) ethanol], resuspended and treated with AMV RTase for 90 min at 42°C following the manufacturer's specifications (Roche Diagnostics, Mannheim, Germany). After a final overnight precipitation and washing step, the pellet was dissolved in 4 μl of DEPC-treated H_2O. The obtained primer extension product was loaded in parallel with a sequencing sample of the *prxS* 5′ region using the same primer on an ALF Express II machine (Amersham Pharmacia Biotech, Freiburg, Germany) and visualized with the Sequence Analyzer 2.10 software.

Plant experiments, acetylene reduction assay and bacteroid isolation

Common bean plants (*P. vulgaris* cv. Limburgse vroege) were cultivated and assayed for nitrogen fixation capacity as described (Dombrecht *et al*., 2002a). Bacteroids were isolated from 3-week-old nodules according to Leyva *et al*. (1990).

Growth experiments in the presence of reactive oxygen species

Bacterial cultures were grown overnight in TY medium after which OD_{600} was adjusted to 0.5, and diluted 100-fold in fresh TY medium. These cultures were challenged for different periods to 2 mM H_2O_2, 2 mM CuOOH, 2 mM tBuOOH or 1 mM methyl viologen (paraquat). The challenged cultures were diluted 100-fold into AMS medium (supplied with 10 mM NH_4Cl and 10 mM mannitol), grown and monitored every hour in a Bioscreen C apparatus (Labsystems, Helsinki, Finland).

Doubling time assay

Bacterial cultures were grown overnight in liquid TY medium after which they were diluted and plated out on YEM plates supplemented with nalidixic acid. Three days later, individual colonies were picked up from the plates, resuspended in 300 μl AMS (supplied with 10 mM succinate and 10 mM NH_4Cl) and diluted 30 times in the same growth medium. Growth was monitored every hour for 3 days in a Bioscreen C apparatus (Labsystems, Helsinki, Finland) after which the growth rate was determined for each individual colony.

Recombinant protein expression and purification

BL21-CodonPlus(DE3)-RP *E. coli* cells were transformed with the pET-24(+) derivatives (Table 2) and grown overnight in LB medium at 37°C. Subcultures were grown to an OD_{600} of 0.8 and than induced with 1 mM IPTG.

Denatured recombinant PrxS-His_6 was obtained as follows. After IPTG induction, cultures were grown for ≥4 h at 37°C. Cells were collected and kept overnight at −20°C. Proteins were harvested and purified over Ni-NTA agarose resin using buffers containing 8 M urea according the QIA*expressionist* manual (Qiagen, Hilden, Germany). Finally, denatured purified proteins were stored in elution buffer (100 mM NaH_2PO_4, 10 mM Tris, 8 M urea, pH 4.5).

For native recombinant PrxS-His_6, cultures were maintained at 4°C for 7 days after IPTG induction. After collection and overnight storage at −20°C, cells were treated with lysozyme and sonicated in native lysis buffer (50 mM Tris, 300 mM NaCl, 10 mM imidazole, pH 8.0) supplemented with 5 mM DTT. Total soluble protein fractions, in which a significant fraction of native PrxS-His_6 was present, were dialysed against native lysis buffer. Native PrxS-His_6 was eluted from Ni-NTA agarose with elution buffer (50 mM Tris, 300 mM NaCl, 250 mM imidazole, pH 8.0) and subsequently dialysed (50 mM Tris, 50 mM NaCl, pH 8.0). The adapted purification protocol was functional for native PrxS, C56S and C156S but we were unable to obtain C81S from the soluble phase. When IPTG-induced cultures were grown at 37°C for 4 h and subsequently treated using native buffers as described above, recombinant PrxS-His_6 was exclusively present in inclusion bodies.

N-terminal amino acid sequencing

N-terminal microsequencing of recombinant PrxS-His_6 was performed as described by Parret *et al.* (2003).

Peroxidase assays

Recombinant PrxS-His_6 and Cys-Ser mutants (2 μM) in buffer (50 mM Tris, 50 mM NaCl, 2 mM DTT, pH 8.0) were incubated at 37°C, after which the reactions were initiated by addition of 2.5 mM peroxide. At different time points, samples were taken and the reaction was terminated by adding 12.5% (w/v) TCA. Peroxide concentration was determined with the ferrithiocyanate assay (Thurman *et al.*, 1972).

The oxidation of NADPH (Sigma-Aldrich) was monitored in the presence of different peroxides, PrxS-His_6 and two different thiol-dependent reducing cascades: thioredoxin reductase (TR)/thioredoxin (Trx) [both from *E. coli* (Sigma-Aldrich)] and glutathione reductase (GR)/oxidized glutathione (GSSG)/glutaredoxin (GRX) [GR from *Saccharomyces cerevisiae*, GRX from *E. coli* (Sigma-Aldrich)]. A typical reaction mixture contained 250 μM NADPH, 0.2 μM TR (or 2 μM GR), 2 μM Trx (or 2 μM GSSG and GRX), 1 μM PrxS and varying (2 μM up to 2 mM) peroxide concentrations. Reactions (37°C, 50 mM Tris, 50 mM NaCl, pH 8.0), were started by addition of peroxides and NADPH oxidation (absorption at 340 nm) was followed on a VERSAmax microplate reader (Molecular Devices). Initial rates were calculated from the slope between 15 s and 45 s after peroxide addition and corrected for background reduction present in reactions lacking PrxS.

Acknowledgements

Jan Verhaert, Annabel Parret, Jos Desair and Istvan Nagy are gratefully acknowledged for their advice on the protein purification schemes, Bernard Knoops for the helpful discussion on peroxiredoxins and the anonymous referees for their useful comments improving the manuscript. B.D. is indebted to the Onderzoeksfonds K.U.Leuven for financial support (PDM/01/116 and PDM/02/144). This work was supported by grants from the Fund for Scientific Research – Flanders (G.0108.01 and G.0287.04) and from the Research Council of the Katholieke Universiteit Leuven (GOA/2003/09).

Supplementary material

The following material is available from http://www.blackwellpublishing.com/products/journals/suppmat/mmi/mmi4457/mmi4457sm.htm

Fig. S1. Three-dimensional model prediction of *Rhizobium etli* PrxS based on homologues of known structure using 3D-Jigsaw (Bates *et al.*, 2001).

References

Ampe, F., Kiss, E., Sabourdy, F., and Batut, J. (2003) Transcriptome analysis of *Sinorhizobium meliloti* during symbiosis. *Genome Biol* **4:** R15.

Baker, L.M.S., and Poole, L.B. (2003) Catalytic mechanism of thiol peroxidase from *Escherichia coli* – sulfenic acid formation and overoxidation of essential CYS61. *J Biol Chem* **278:** 9203–9211.

Barrios, H., Valderrama, B., and Morett, E. (1999) Compilation and analysis of sigma 54-dependent promoter sequences. *Nucleic Acids Res* **27:** 4305–4313.

Bates, P.A., Kelley, L.A., MacCallum, R.M., and Sternberg, M.J. (2001) Enhancement of protein modeling by human intervention in applying the automatic programs 3D-JIGSAW and 3D-PSSM. *Proteins* **Suppl. 5:** 39–46.

Becana, M., Dalton, D.A., Moran, J.F., Iturbe, O.I., Matamoros, M.A., and Rubio, M.C. (2000) Reactive oxygen species and antioxidants in legume nodules. *Physiologia Plantarum* **109:** 372–381.

Choi, J.K., Choi, S., Choi, J.W., Cha, M.K., Kim, I.H., and Shin, W. (2003) Crystal structure of *Escherichia coli* thiol peroxidase in the oxidized state – insights into intramo-

lecular disulfide formation and substrate binding in atypical 2-Cys peroxiredoxins. *J Biol Chem* **278:** 49478–49486.

Crockford, A.J., Davis, G.A., and Williams, H.D. (1995) Evidence for cell-density-dependent regulation of catalase activity in *Rhizobium leguminosarum* bv. *phaseoli*. *Microbiology* **141:** 843–851.

Cullen, P.J., Foster-Hartnett, D., Gabbert, K.K., and Kranz, R.G. (1994) Structure and expression of the alternative sigma factor, RpoN, in *Rhodobacter capsulatus*; physiological relevance of an autoactivated *nifU$_2$-rpoN* superoperon. *Mol Microbiol* **11:** 51–65.

Cullimore, J.V., Ranjeva, R., and Bono, J.J. (2001) Perception of lipo-chitooligosaccharidic Nod factors in legumes. *Trends Plant Sci* **6:** 24–30.

D'Haeze, W., and Holsters, M. (2002) Nod factor structures, responses, and perception during initiation of nodule development. *Glycobiology* **12:** 79R–105R.

D'Haeze, W., De Rycke, R., Mathis, R., Goormachtig, S., Pagnotta, S., Verplancke, C., *et al.* (2003) Reactive oxygen species and ethylene play a positive role in lateral root base nodulation of a semiaquatic legume. *Proc Natl Acad Sci USA* **100:** 11789–11794.

Declercq, J.P., Evrard, C., Clippe, A., Stricht, D.V., Bernard, A., and Knoops, B. (2001) Crystal structure of human peroxiredoxin 5, a novel type of mammalian peroxiredoxin at 1.5 A resolution. *J Mol Biol* **311:** 751–759.

Djordjevic, M.A., Chen, H.C., Natera, S., Van Noorden, G., Menzel, C., Taylor, S., *et al.* (2003) A global analysis of protein expression profiles in *Sinorhizobium meliloti*: discovery of new genes for nodule occupancy and stress adaptation. *Mol Plant Microbe Interact* **16:** 508–524.

Dombrecht, B., Vanderleyden, J., and Michiels, J. (2001) Stable RK2-derived cloning vectors for the analysis of gene expression and gene function in gram-negative bacteria. *Mol Plant Microbe Interact* **14:** 426–430.

Dombrecht, B., Tesfay, M.Z., Verreth, C., Heusdens, C., Napoles, M.C., Vanderleyden, J., and Michiels, J. (2002a) The *Rhizobium etli* gene *iscN* is highly expressed in bacteroids and required for nitrogen fixation. *Mol Genet Genom* **267:** 820–828.

Dombrecht, B., Marchal, K., Vanderleyden, J., and Michiels, J. (2002b) Prediction and overview of the RpoN-regulon in closely related species of the *Rhizobiales*. *Genome Biol* **3:** RESEARCH0076.

Eggermont, K., Goderis, I.J., and Broekaert, W.F. (1996) High-throughput RNA extraction from plant samples based on homogenisation by reciprocal shaking in the presence of a mixture of sand and glass beads. *Plant Mol Biol Rep* **14:** 273–279.

Fellay, R., Frey, J., and Krisch, H. (1987) Interposon mutagenesis of soil and water bacteria: a family of DNA fragments designed for *in vitro* insertional mutagenesis of gram-negative bacteria. *Gene* **52:** 147–154.

Figurski, D.H., and Helinski, D.R. (1979) Replication of an origin-containing derivative of plasmid RK2 dependent on a plasmid function provided *in trans*. *Proc Natl Acad Sci USA* **76:** 1648–1652.

Fraysse, N., Couderc, F., and Poinsot, V. (2003) Surface polysaccharide involvement in establishing the rhizobium-legume symbiosis. *Eur J Biochem* **270:** 1365–1380.

Freiberg, C., Fellay, R., Bairoch, A., Broughton, W.J., Rosenthal, A., and Perret, X. (1997) Molecular basis of symbiosis between *Rhizobium* and legumes. *Nature* **387:** 394–401.

Galibert, F., Finan, T.M., Long, S.R., Puhler, A., Abola, P., Ampe, F., *et al.* (2001) The composite genome of the legume symbiont *Sinorhizobium meliloti*. *Science* **293:** 668–672.

Gonzalez, V., Bustos, P., Ramirez-Romero, M.A., Medrano-Soto, A., Salgado, H., Hernandez-Gonzalez, I., *et al.* (2003) The mosaic structure of the symbiotic plasmid of *Rhizobium etli* CFN42 and its relation to other symbiotic genome compartments. *Genome Biol* **4:** R36.

Herouart, D., Sigaud, S., Moreau, S., Frendo, P., Touati, D., and Puppo, A. (1996) Cloning and characterization of the *katA* gene of *Rhizobium meliloti* encoding a hydrogen peroxide-inducible catalase. *J Bacteriol* **178:** 6802–6809.

Herouart, D., Baudouin, E., Frendo, P., Harrison, J., Santos, R., Jamet, A., *et al.* (2002) Reactive oxygen species, nitric oxide and glutathione: a key role in the establishment of the legume–*Rhizobium* symbiosis? *Plant Physiol Biochem* **40:** 619–624.

Hofmann, B., Hecht, H.J., and Flohe, L. (2002) Peroxiredoxins. *Biol Chem* **383:** 347–364.

Jamet, A., Sigaud, S., Van de Sype, G., Puppo, A., and Herouart, D. (2003) Expression of the bacterial catalase genes during *Sinorhizobium meliloti–Medicago sativa* symbiosis and their crucial role during the infection process. *Mol Plant Microbe Interact* **16:** 217–225.

Kaneko, T., Nakamura, Y., Sato, S., Asamizu, E., Kato, T., Sasamoto, S., *et al.* (2000) Complete genome structure of the nitrogen-fixing symbiotic bacterium *Mesorhizobium loti*. *DNA Res* **7:** 331–338.

Kim, S.J., Woo, J.R., Hwang, Y.S., Jeong, D.G., Shin, D.H., Kim, K., and Ryu, S.E. (2003) The tetrameric structure of *Haemophilus influenza* hybrid Prx5 reveals interactions between electron donor and acceptor proteins. *J Biol Chem* **278:** 10790–10798.

Kobayashi, M., Ishizuka, T., Katayama, M., Kanehisa, M., Bhattacharyya-Pakrasi, M., Pakrasi, H.B., and Ikeuchi, M. (2004) Response to oxidative stress involves a novel peroxiredoxin gene in the unicellular cyanobacterium *Synechocystis* sp PCC 6803. *Plant Cell Physiol* **45:** 290–299.

Leyva, A., Palacios, J.M., Murillo, J., and Ruiz-Argueso, T. (1990) Genetic organization of the hydrogen uptake (*hup*) cluster from *Rhizobium leguminosarum*. *J Bacteriol* **172:** 1647–1655.

Li, H., Rhodius, V., Gross, C., and Siggia, E.D. (2002) Identification of the binding sites of regulatory proteins in bacterial genomes. *Proc Natl Acad Sci USA* **99:** 11772–11777.

Matamoros, M.A., Dalton, D.A., Ramos, J., Clemente, M.R., Rubio, M.C., and Becana, M. (2003) Biochemistry and molecular biology of antioxidants in the rhizobia-legume symbiosis. *Plant Physiol* **133:** 499–509.

Michiels, J., D'hooghe, I., Verreth, C., Pelemans, H., and Vanderleyden, J. (1994) Characterization of the *Rhizobium leguminosarum* biovar *phaseoli nifA* gene, a positive regulator of *nif* gene expression. *Arch Microbiol* **161:** 404–408.

Michiels, J., Moris, M., Dombrecht, B., Verreth, C., and Vanderleyden, J. (1998a) Differential regulation of *Rhizo-*

bium etli rpoN$_2$ gene expression during symbiosis and free-living growth. *J Bacteriol* **180:** 3620–3628.

Michiels, J., Van Soom, T., D'hooghe, I., Dombrecht, B., Benhassine, T., de Wilde, P., and Vanderleyden, J. (1998b) The *Rhizobium etli rpoN* locus: DNA sequence analysis and phenotypical characterization of *rpoN*, *ptsN*, and *ptsA* mutants. *J Bacteriol* **180:** 1729–1740.

Mithofer, A. (2002) Suppression of plant defence in rhizobia-legume symbiosis. *Trends Plant Sci* **7:** 440–444.

Mongkolsuk, S., and Helmann, J.D. (2002) Regulation of inducible peroxide stress responses. *Mol Microbiol* **45:** 9–15.

Moran, J.F., Iturbe-Ormaetxe, I., Matamoros, M.A., Rubio, M.C., Clemente, M.R., Brewin, N.J., and Becana, M. (2000) Glutathione and homoglutathione synthetases of legume nodules. Cloning, expression, and subcellular localization. *Plant Physiol* **124:** 1381–1392.

Moreno, S., Patriarca, E.J., Chiurazzi, M., Meza, R., Defez, R., Lamberti, A., *et al.* (1992) Phenotype of a *Rhizobium leguminosarum ntrC* mutant. *Res Microbiol* **143:** 161–171.

Ohwada, T., Shirakawa, Y., Kusumoto, M., Masuda, H., and Sato, T. (1999) Susceptibility to hydrogen peroxide and catalase activity of root nodule bacteria. *Biosci Biotechnol Biochem* **63:** 457–462.

Oke, V., and Long, S.R. (1999) Bacterial genes induced within the nodule during the *Rhizobium*-legume symbiosis. *Mol Microbiol* **32:** 837–849.

Parret, A.H., Schoofs, G., Proost, P., and De Mot, R. (2003) Plant lectin-like bacteriocin from a rhizosphere-colonizing *Pseudomonas* isolate. *J Bacteriol* **185:** 897–908.

Patriarca, E.J., Tate, R., Fedorova, E., Riccio, A., Defez, R., and Laccarino, M. (1996) Down-regulation of the *Rhizobium ntr* system in the determinate nodule of *Phaseolus vulgaris* identifies a specific developmental zone. *Mol Plant Microbe Interact* **9:** 243–251.

Patriarca, E.J., Tate, R., and Laccarino, M. (2002) Key role of bacterial NH(4)(+) metabolism in *Rhizobium*–plant symbiosis. *Microbiol Mol Biol Rev* **66:** 203–222.

Perret, X., Freiberg, C., Rosenthal, A., Broughton, W.J., and Fellay, R. (1999) High-resolution transcriptional analysis of the symbiotic plasmid of *Rhizobium* sp. NGR234. *Mol Microbiol* **32:** 415–425.

Poole, L.B., Reynolds, C.M., Wood, Z.A., Karplus, P.A., Ellis, H.R., and Calzi, M.L. (2000) AhpF and other NADH: peroxiredoxin oxidoreductases, homologues of low M-r thioredoxin reductase. *Eur J Biochem* **267:** 6126–6133.

Poole, P.S., Schofield, N.A., Reid, C.J., Drew, E.M., and Walshaw, D.L. (1994) Identification of chromosomal genes located downstream of *dctD* that affect the requirement for calcium and the lipopolysaccharide layer of *Rhizobium leguminosarum*. *Microbiology* **140:** 2797–2809.

Quandt, J., and Hynes, M.F. (1993) Versatile suicide vectors which allow direct selection for gene replacement in gram-negative bacteria. *Gene* **127:** 15–21.

Santos, R., Herouart, D., Puppo, A., and Touati, D. (2000) Critical protective role of bacterial superoxide dismutase in *Rhizobium*-legume symbiosis. *Mol Microbiol* **38:** 750–759.

Santos, R., Herouart, D., Sigaud, S., Touati, D., and Puppo, A. (2001) Oxidative burst in alfalfa–*Sinorhizobium meliloti* symbiotic interaction. *Mol Plant Microbe Interact* **14:** 86–89.

Schmehl, M., Jahn, A., Vilsendorf, A.M.Z., Hennecke, S., Masepohl, B., Schuppler, M., *et al.* (1993) Identification of a new class of nitrogen-fixation genes in *Rhodobacter capsulatus* a putative membrane complex involved in electron-transport to nitrogenase. *Mol Gen Genet* **241:** 602–615.

Schwede, T., Kopp, J., Guex, N., and Peitsch, M.C. (2003) SWISS-MODEL: an automated protein homology-modeling server. *Nucleic Acids Res* **31:** 3381–3385.

Seo, M.S., Kang, S.W., Kim, K., Baines, I.C., Lee, T.H., and Rhee, S.G. (2000) Identification of a new type of mammalian peroxiredoxin that forms an intramolecular disulfide as a reaction intermediate. *J Biol Chem* **275:** 20346–20354.

Shaw, S.L., and Long, S.R. (2003) Nod factor inhibition of reactive oxygen efflux in a host legume. *Plant Physiol* **132:** 2196–2204.

Sigaud, S., Becquet, V., Frendo, P., Puppo, A., and Herouart, D. (1999) Differential regulation of two divergent *Sinorhizobium meliloti* genes for HPII-like catalases during free-living growth and protective role of both catalases during symbiosis. *J Bacteriol* **181:** 2634–2639.

Sullivan, J.T., Trzebiatowski, J.R., Cruickshank, R.W., Gouzy, J., Brown, S.D., Elliot, R.M., *et al.* (2002) Comparative sequence analysis of the symbiosis island of *Mesorhizobium loti* strain R7A. *J Bacteriol* **184:** 3086–3095.

Thurman, R.G., Ley, H.G., and Scholz, R. (1972) Hepatic microsomal ethanol oxidation. Hydrogen peroxide formation and the role of catalase. *Eur J Biochem* **25:** 420–430.

Vargas, M.C., Encarnacion, S., Davalos, A., Reyes-Perez, A., Mora, Y., Garcia-de los Santos, A., *et al.* (2003) Only one catalase, *katG*, is detectable in *Rhizobium etli*, and is encoded along with the regulator OxyR on a plasmid replicon. *Microbiology* **149:** 1165–1176.

Vincent, J.M. (1970) *A Manual for the Practical Study of the Root-Nodule Bacteria.* Oxford: Blackwell Scientific Publications.

Wisniewski, J.P., Rathbun, E.A., Knox, J.P., and Brewin, N.J. (2000) Involvement of diamine oxidase and peroxidase in insolubilization of the extracellular matrix: implications for pea nodule initiation by *Rhizobium leguminosarum*. *Mol Plant Microbe Interact* **13:** 413–420.

Wood, D.W., Setubal, J.C., Kaul, R., Monks, D.E., Kitajima, J.P., Okura, V.K., *et al.* (2001) The genome of the natural genetic engineer *Agrobacterium tumefaciens* C58. *Science* **294:** 2317–2323.

Wood, Z.A., Schroder, E., Robin, H.J., and Poole, L.B. (2003) Structure, mechanism and regulation of peroxiredoxins. *Trends Biochem Sci* **28:** 32–40.

Xi, C., Schoeters, E., Vanderleyden, J., and Michiels, J. (2000) Symbiosis-specific expression of *Rhizobium etli casA* encoding a secreted calmodulin-related protein. *Proc Natl Acad Sci USA* **97:** 11114–11119.

Xi, C., Dirix, G., Hofkens, J., Schryver, F.C., Vanderleyden, J., and Michiels, J. (2001) Use of dual marker transposons to identify new symbiosis genes in *Rhizobium*. *Microb Ecol* **41:** 325–332.

Zheng, M., Wang, X., Templeton, L.J., Smulski, D.R., LaRossa, R.A., and Storz, G. (2001) DNA microarray-mediated transcriptional profiling of the *Escherichia coli* response to hydrogen peroxide. *J Bacteriol* **183:** 4562–4570.